Analytical and Bioanalytical Chemistry (2021) 413:4989–5001
https://doi.org/10.1007/s00216-021-03460-y

RESEARCH PAPER

Site-specific glycan-conjugated NISTmAb antibody drug conjugate mimetics: synthesis, characterization, and utility

Brian Agnew[1] · Shanhua Lin[2] · Terry Zhang[2] · Robert Aggeler[1] · Trina Mouchahoir[3] · John Schiel[3]

Received: 8 February 2021 / Revised: 1 June 2021 / Accepted: 8 June 2021 / Published online: 6 July 2021
© This is a U.S. government work and not under copyright protection in the U.S.; foreign copyright protection may apply 2021

Abstract

Antibody drug conjugates (ADCs) represent a rapidly growing modality for the treatment of numerous oncology indications. The complexity of analytical characterization method development is increased due to the potential for synthetic intermediates and process-related impurities. In addition, the cytotoxicity of such materials provides an additional challenge with regard to handling products and/or sharing materials with analytical collaborators and/or vendors for technology development. Herein, we have utilized a site-specific chemoenzymatic glycoconjugation strategy for preparing ADC mimetics composed of the NIST monoclonal antibody (NISTmAb) conjugated to non-cytotoxic payloads representing both small molecules and peptides. The materials were exhaustively characterized with high-resolution mass spectrometry-based approaches to demonstrate the utility of each analytical method for confirming the conjugation fidelity as well as deep characterization of low-abundance synthetic intermediates and impurities arising from payload raw material heterogeneity. These materials therefore represent a widely available test metric to develop novel ADC analytical methods as well as a platform to discuss best practices for extensive characterization.

Keywords Antibody drug conjugate · NISTmAb · Monoclonal antibody · Biotherapeutic · Biopharmaceutical · System suitability

Introduction

Successful development of innovative therapeutic modalities requires a complex interplay between process development and analytical/biophysical characterization technologies to inform on product quality attributes (PQAs). Antibody drug conjugates (ADCs) are an emerging class of therapeutics whose characterization and control strategy challenges continue to emerge as innovative products come to market. Measurement science associated with emerging modalities such as ADCs can be greatly improved through a variety of mechanisms including industrial consortia, peer-reviewed publications, and pre-competitive test cases. The NIST monoclonal antibody (NISTmAb) RM 8671 is an example wherein a publicly available and highly characterized material can serve as a biopharmaceutical industry standard to accelerate innovation [1–5]. The NISTmAb has been used for demonstrating new technologies including nuclear magnetic resonance (NMR), neutron scattering, and numerous mass spectrometry-based approaches, among others [6–20]. The pre-competitive nature of the NISTmAb has also proven useful as a framework to evaluate method/technology performance through comparative inter-laboratory studies [7]. The collective information is imperative to facilitate industry-wide

NIST Disclaimer: Values reported herein do not supersede official NISTmAb Report of Investigation and are for informational purposes only. Users should always refer to the Report of Investigation (https://www-s.nist.gov/srmors/view_detail.cfm?srm=8671) for their specific material lot for the most up to date values and uncertainty ranges. Certain commercial equipment, instruments, or materials are identified to adequately specify the experimental procedure. Such identification does not imply recommendation or endorsement by the National Institute of Standards and Technology, nor does it imply that the materials or equipment identified are necessarily the best available for the purpose.

✉ Brian Agnew
brian.agnew@thermofisher.com

✉ John Schiel
john.schiel@nist.gov

[1] Biosciences Division, Thermo Fisher Scientific, 29851 Willow Creek Road, Eugene, OR 97402, USA

[2] Chromatography Columns and Consumables, Thermo Fisher Scientific, Sunnyvale, CA 94085, USA

[3] Institute for Bioscience and Biotechnology Research, National Institute of Standards and Technology, 9600 Gudelsky Dr, Rockville, MD 20850, USA

best practices for lifecycle appropriate implementation of new analytical methods for characterization, process monitoring, quality control, and/or comparability and biosimilarity. NISTmAb ADC mimetic molecules and/or robust established protocols for their creation would serve a similar purpose for tackling the unique analytical challenges associated with this emerging therapeutic class.

Antibody drug conjugates are composed of a monoclonal antibody framework conjugated with small molecule or peptide cytotoxic drug payloads [21, 22]. The antibody serves as a molecular homing device by binding with high affinity and specificity to a tissue-specific marker (e.g., tumor antigen). The ADC complex is then internalized via the phagocytic pathway into lysozymes for degradation which, in turn, releases the toxic payload molecules for a cancer cell-selective delivery [23]. This mechanism of action (MOA) requires the monoclonal antibody, linker chemistry, and payload to work in harmony to elicit a functional outcome.

Ten ADCs are currently approved by the US FDA using a variety of conjugation/linker chemistry strategies including ado-trastuzumab emtansine (Kadcyla™), brentuximab vedotin (Adcetris™), inotuzumab ozogamicin (Besponsa™), gemtuzumab ozogamicin (Mylotarg™), polatuzumab vedotin-piiq (Polivy™), enfortumab vedotin (Padcev™), trastuzumab deruxtecan (Enhertu™), sacituzumab govitecan (Trodelvy™), moxetumomab pasudotox (Lumoxiti™), and belantamab mafodotin (Blenrep). Adcetris and Kadcyla are based on IgG1 constructs while Besponsa and Mylotarg utilize IgG4. Kadcyla utilizes lysine conjugation via a non-cleavable thioether-containing linker. Adcetris is a cysteine-conjugated ADC that utilizes a protease cleavable linker. Besponsa and Mylotarg have their payload attached to lysine residues using a linker with both acid cleavable (hydrazide) and reducible (disulfide) groups. In 2019 alone, U.S. regulators approved three ADCs, the most ever in a single year. They include AstraZeneca's and Daiichi Sankyo's breast cancer drug Enhertu, Astellas' and Seattle Genetics' bladder cancer drug, Padcev, and Roche's Polivy, targeted against lymphoma. Additionally, Immunomedics' Trodelvy for treatment of triple-negative breast cancer and GalaxoSmithKline's, Blenrep, for treatment of refractory multiple myeloma, were most recently approved in 2020.

With the exception of Polivy, each of the FDA-approved ADCs utilizes pre-existing amino acids (either partial cysteine reduction or free lysine conjugation), resulting in a distribution of antibody molecules with varying numbers of attached payloads with average DAR values reported on each of the drug's labels ranging from 2 to 6. Recent trends in ADC development, however, have steered toward using engineered non-native free cysteine or other biorthogonal residues for ADC linkage, or chemoenzymatic engineering of native antibodies. To date, the only FDA-approved ADC utilizing site-specific conjugation is polatuzumab-vedotin (Polivy®), a humanized monoclonal antibody produced using a site-specific covalent bond conjugated via engineered cysteines (THIOMABs). However, more than 50% of the estimated 90 antibodies currently in clinical trials utilize site-specific conjugation methods, and in 2020, all antibodies entering the clinic utilize site-specific conjugation [24, 25].

Drug payloads can be attached to the antibody via a number of naturally occurring amino acids, non-native amino acids, glycans, etc. (Table 1) [21]. Conjugation using native cysteine residues often requires partial reduction of interchain disulfides to the free thiol form prior to conjugation, resulting in heterogeneous incorporation of up to 8 payloads per molecule [26]. Conjugation via primary amine residues present on lysine and the N-termini has also been utilized. Using this strategy, conjugation can be limited to surface-exposed residues resulting in incorporation of multiple payloads to per IgG. Conjugation to native cysteine and lysine residues both lead to a heterogeneous population of individual IgG species with a different number of payloads which may in turn result in different physicochemical and pharmacokinetic properties. In both scenarios, reaction conditions must be controlled to produce a consistent average drug to antibody ratio (DAR) incorporation.

Site-specific conjugation strategies have become an increasingly popular development strategy in an effort to minimize product heterogeneity. Site-specific incorporation enables conjugation at defined sites, typically distant from the antigen-binding domains to minimize impact to antigen recognition. Examples of site-specific incorporation methods include genetic incorporation of nascent cysteine residues to yield free thiols for chemical conjugation, genetic engineering of unnatural amino acids containing bio-orthogonal reactive groups (e.g., thiols, azides, or keto groups) for use in chemical conjugation, and conjugation via chemoenzymatic engineering of naked antibodies with reactive biorthogonal species. One major benefit of using biorthogonal chemoenzymatic approach is that it does not require any genetic engineering and can be used with essentially any preexisting antibodies. Each of these strategies provides an opportunity for homogenous payload incorporation of a specific number of payloads per IgG molecule assuming complete reaction. The advantages of site-specific conjugation have recently been demonstrated and include marked improvement over non-site-specific methods including enhanced plasma stability, enhanced tumor uptake, improved binding efficiency, increased antigen binding, and less variability in dosing studies [25].

Desired quality characteristics of the antibody framework share many common traits with standalone large

Table 1 Potential conjugation chemistries for antibody drug conjugate synthesis

Residue	Chemistry	[a]Number of payloads per molecule	[b]Maximum # conjugation sites in NISTmAb
Native cysteine	Partial reduction of disulfides	0 to 8	16 disulfides
Lysine + N-termini	Amide formation	0 to 10	92 lysines 4 N-termini
Non-native cysteine	Free cysteine	# free cysteines (typically 2)	0
Bio-orthogonal amino acid	Dependent on amino acid	# of bio-orthogonal AAs (typically 2-4)	0
Glycan	Chemoenzymatic	2-6	2

[a] Value of 2 for site-specific conjugation strategies assumes complete synthetic yield

[b] Maximum number of conjugation sites in NISTmAb refers to all sites present based on the primary amino acid sequence without consideration of potential steric accessibility considerations

molecule counterparts, reviewed in detail elsewhere [19]. In fact, comprehensive elucidation of structure of the antibody is required for regulatory approval. Modification of the antibody with payload molecules adds an extra dimension of complexity that may alter antibody physicochemical characteristics [27, 28], and therefore an extensive analytical package must also be applied to final ADC products. Implementation of the most advanced analytical technologies, from primary to higher order structure, is critical to fully understand the potential impacts of conjugation on product quality. Moreover, the drug to antibody ratio is a critical quality attribute shared by all ADCs that absolutely must be controlled for consistent product safety and efficacy. Analytical methods for DAR determination are many, including various mass spectrometry-based approaches (intact, subunit mass, and/or peptide mapping) as well as chromatographic methods such as hydrophobic interaction chromatography. It would be highly desirable to have ADC mimetics for innovative ADC analytical technology development as well as in-depth evaluation of DAR method figures of merit, much as NISTmAb has done for antibody therapeutics.

Chemoenzymatic glycan modification of the NISTmAb RM 8671 was utilized herein to prepare ADC mimetics based on conjugation of various non-toxic payloads (Alexa Fluor 488, biotin, and angiotensin II) to the NISTmAb. This synthetic approach was selected in an attempt to prepare site-specifically conjugated, non-toxic, DAR ≈ 2, ADC mimetics to resemble the industry trending direction. A series of analytical characterization assays were performed on each of the mimetics to evaluate synthetic fidelity as well as product quality attributes. The NISTmAb ADC mimetics represent novel analytical materials and the associated preparation/characterization strategy may serve as a guideline for development of related protocols/materials with orthogonal properties.

Materials and methods

NISTmAb azide activation Unless otherwise stated, all modification steps in the NISTmAb conjugation procedures were performed using the NISTmAb storage buffer, 25 mmol/L L-His (His) buffer, pH 6.0. An 8-mg vial of NISTmAb (NIST) (10 mg/mL) was thawed on ice and adjusted to 1800 μL with 25 mmol/L His buffer, pH 6.0. In total, 200 μL of EndoS2 (Glycinator, Genovis) was added and the solution was incubated for 3 h at 37 °C. Final Ab concentration was ≈4 mg/mL. After EndoS2 treatment, chemoenzymatic modification of the NISTmAb N-linked core GlcNAc sugar residues (resulting from EndoS2 cleavage) was azide-activated by the addition of GalT(Y289L) mutant enzyme, UDP-GalNAz, and $MnCl_2$. The reaction mix was incubated while rotating at 30 °C for 16 h. After incubation, the reaction components were removed by using 4 mL 50 kD Amicon Ultra spin filters and performing 6 full washes in 25 mmol/L His buffer, pH 6.0. After the last wash, the antibody was brought to a final volume of 4 mL (≈2.0 mg/mL). Post-labeling, 100 μg of the antibody was removed and reacted with Alexa Fluor 488 dye as a standard test for DOL determination. The antibody was incubated overnight (16 h) and the free dye was removed using 0.5 mL 50 kD cutoff Amicon Ultra spin filters with 5 washes. The DOL was calculated by measuring absorbances at A280 and A496 and applying the corresponding extinction coefficients for the antibody and the dye, respectively. The final DOL of the azide-activated antibody using the spectroscopic method was calculated to be 2.1.

NISTmAb ADC conjugation Azide-activated NISTmAb (NISTmAb-N_3, 2 mg/mL final) was conjugated with sDIBO-Alexa Fluor 488 dye, sDIBO-Biotin, or sDIBO-Angiotensin II peptide (sDIBO-ATII) copperless click cyclooctyne compounds (Thermo Fisher Scientific) (0.2 mmol/L final) in His buffer, pH 6.0 for 16 h. After incubation, the free unreacted sDIBO compounds were removed using 4

mL 50 kD Amicon Ultra spin filters and performing 6 full washes in 25 mmol/L His Buffer, pH 6.0.

NISTmAb ADC preparation for mass spectrometric analyses In preparation for mass spectrometry analysis, the antibodies were exhaustively dialyzed into ammonium acetate buffer, dried down in the speed vac, and submitted for analysis. For Fab and single-chain Fc (scFc) fragment analysis, the antibodies were cleaved using Frag-iT microspin columns (Genovis, Sweden) and buffer exchanged in 0.5 mL 10 kD cutoff Amicon Ultra spin filters and dried in the speed vac.

Intact and middle-down mass spectrometry Intact and fragment samples were separated and analyzed on Thermo Scientific™ Vanquish™ UHPLC system, using a MAbPac RP analytical column, 4.0 μm, 2.1 × 50 mm column (p/n 088648) at 80 °C. When coupling UHPLC with a UV detector, H_2O/trifluoroacetic acid/acetonitrile mobile phase was used. When coupling UHPLC with Orbitrap Fusion Lumos Tribrid Mass Spectrometer instrument, H_2O/formic acid/acetonitrile mobile phase was used. The MS acquisition method was set with a full scan at both 15,000 (FWHM, at *m/z* 200) and 120,000 resolution in positive mode. The method parameters were as follows: AGC 2E5, IT 200 ms, in-source CID 0 eV and 35 eV, scan range 800–3000, 1000–3500 *m/z*, spray voltage 3.8 kV, sheath gas 60, aux gas 20, capillary temperature 350 °C, s-lens 30, probe heater temperature 150 °C.

Peptide mapping Tryptic digestion of RM 8671 and all ADC mimetics was performed according to the procedure described previously with minor modification [1]. Minor modifications included direct buffer exchange to 10.1 % v/v formulation buffer (25 mmol/L L-His, pH 6.0), 89.9 % v/v denaturing buffer (6 mol/L Guanidine HCl, 100 mmol/L pH 7.8 Tris, and 1 mmol/L EDTA), reduced and alkylated as previously reported [1], and samples were digested at a slightly lower total antibody concentration (0.24 μg/μL) in 1 mol/L urea. Peptide mapping using reversed phase ultrahigh-performance liquid chromatography coupled to UV-visible and tandem mass spectrometry detection (LC-UV-MS/MS) was used to confirm the primary amino acid sequence, evaluate conjugation efficiency, and determine post-translational modification (PTM) relative abundance. Liquid chromatography was performed using the Dionex UltiMate™ Rapid Separation Binary Pump (P/N HPG-3200RS), coupled to a thermostatted rapid separation well plate autosampler (P/N WPS-3000TRS), thermostatted column oven (P/N TCC-3000RS), and variable wavelength detector (P/N VWD-3400RS) manufactured by Thermo Scientific (Waltham, MA). Mass spectrometry analyses were performed using the LTQ Orbitrap Elite with heated electrospray ionization source probe (HESI-II) manufactured by Thermo Scientific. The instruments were controlled using Xcalibur 2.1.0 SP1 Build 1160 (Thermo Scientific, Waltham, MA) and Dionex Chromatography MS Link (DCMS Link) for Xcalibur 2.14 Build 3818 (Thermo Scientific, Waltham, MA).

A total of 3 μg (25 μL) of peptide digests were loaded via autosampler onto a C18 column (Agilent Zorbax RRHD StableBond C18 column, 300 Å, 2.1 mm × 150 mm, 1.8 μm; Manufacturer Part # 863750-902) enclosed in a thermostatted column oven set to 50 °C. Samples were held at 6 °C while queued for injection. The chromatographic method is described in Supplementary Information (ESM) Table S1. Peptides eluting from the chromatography column were analyzed by UV absorption at 214 nm followed by mass spectrometry on the LTQ Orbitrap Elite.

The MS/MS analyses were performed for peptide identification in data-dependent mode in which one cycle of experiments consisted of one full MS scan of 300 to 2000 *m/z* followed by five sequential MS/MS events performed on the first through fifth most intense ions detected at a minimum threshold count of 500 in the MS scan initiating that cycle. Full MS scans were collected in profile mode using the high-resolution FTMS analyzer (R = 60,000) with a full scan AGC target of 1E6 and microscans = 1. The MSn AGC target was set to 3E4 with microscans = 1. The ion trap was used in centroid mode at normal scan rate to analyze MS/MS fragments.

Ions were selected for MS/MS using an isolation width of 2 Da, then fragmented by collision induced dissociation (CID) with helium gas using a normalized CID energy of 35, an activation Q of 0.25 and an activation time of 10 ms. A default charge state was set at z = 2. Data-dependent masses were placed on the exclusion list for 10 s if the precursor ion triggered a single event; the exclusion mass width was set at ± 0.01 %. Charge state rejection was enabled for unassigned charge states. A rejection mass list included common contaminants at 122.0 *m/z*, 185.9 *m/z*, 355.0 *m/z*, 371.0 *m/z*, 391.0 *m/z*, 413.30 *m/z*, 777.7 *m/z*, 803.10 *m/z*, 1222.0 *m/z*, 1322.0 *m/z*, 1422.0 *m/z*, 1522.0 *m/z*, 1622.0 *m/z*, 1722.0 *m/z*, 1822.0 *m/z*, and 1922.0 *m/z*.

LC-MS data analysis was performed using Genedata Expressionist Version 11.0.1. Search parameters included a parent ion mass tolerance of 15 ppm and a fragment mass tolerance of 0.5 Da. Fragmentation spectra were searched using a fixed carbamidomethyl modification and common variable modifications of ammonia loss, Asn deamidation, Met oxidation, N-terminal pyroglutamate, and loss of C-terminal lysine. The default CHO-N-glycan library was searched as a variable modification to detect the presence of any unreleased glycans. Expected ADC conjugate masses were also searched as variable modifications: Alexa Fluor (1740.4678 Da and 1594.41 Da), Angiotensin uncleaved (2297.98 Da and 2151.922 Da), Angiotensin cleaved at the tryptic site (1540.576 Da and 1394.518 Da), Biotin

(1450.552 Da and 1304.494 Da), GalNaz (593.218 Da and 447.1604 Da). Due to the synthetic route for the chemoenzymatic glycosylation, HexNacdHex and Hex were also searched as potential variable modifications on Asn. All MS/MS matches were manually reviewed. Extracted ion relative abundance values were calculated in Genedata Expressionist® using all peptides identified containing a given modification and including adducts (H, K, and Na), all observed charge states, and all observed isotopes.

Results

Each of the ADC mimics was synthesized using the same chemoenzymatic synthesis strategy depicted in Fig. 1. The NISTmAb is composed primarily of complex-type fucosylated biantennary glycans, with a low abundance (approx. 1% each) of Man5, afucosylated complex biantennary, and aglycosylated species [15, 29]. The initial ADC mimic synthetic step involved selectively removing the glycan heterogeneity via enzymatic cleavage of the NISTmAb Fc glycans using Endo-N-acetylglucosaminidase S2 (EndoS2). EndoS2 is capable of selectively cleaving the core GlcNAc-GlcNAc to reveal the GlcNAc-Fuc core (in the case of fucosylated glycans) and a low abundance of GlcNAc-only core (in the case of afucosylated glycans) [30]. The resulting EndoS2-treated substrate will have two potential conjugation sites per antibody, NISTmAb-$Fuc_2GlcNAc_2$ or $GlcNAc_2$, as well as a low abundance of residual afucosylated species equivalent to the original composition of the NISTmAb starting material. The second synthetic step utilizes a mutant β-Galactosyltransferase enzyme (GalT(Y289L)) that has been engineered to have a Y to L point mutation at position 289 to confer a modified substrate transferase activity [31]. GalT(Y289L) efficiently transfers addition of uridine diphosphate activated GalNAz (UDP-GalNAz) via simple hydrolysis to result in an azide-activated mAb with 2 azide residues, one on each heavy chain (NISTmAb-N_3). Copperless click chemistry (as described in "Materials and methods") is then performed to attach 2 of the payload mimics depicted in Fig. 1 which will be referred to by their payload names: Angiotensin II (ATII-mAb), Biotin (Biotin-mAb), and Alexa Fluor 488 (AF488-mAb). Samples from each stage of the reaction scheme were retained for analysis by intact mass spectrometry, middle-down mass spectrometry following IdeS treatment, and LC-MS/MS peptide mapping.

Intact mass spectrometry Intact mass spectrometry is a high-resolution technique capable of measuring monoclonal antibody accurate mass. The LC-UV and deconvoluted mass spectra from the LC-MS analysis for the NISTmAb, synthesis intermediates, and each ADC mimic are shown in Fig. 2. The NISTmAb chromatogram (Fig. 2a) shows a major peak along with a smaller front peak. The deconvoluted spectra of the main NISTmAb peak identified all major glycoforms previously reported for intact NISTmAb to within 15 ppm (ESM Table S2). The NISTmAb-N_3 reaction intermediate shows chromatography similar to the NISTmAb, yet the intact mass spectrum is more homogeneous showing predominantly the desired NISTmAb with two core fucosylated GalNAz

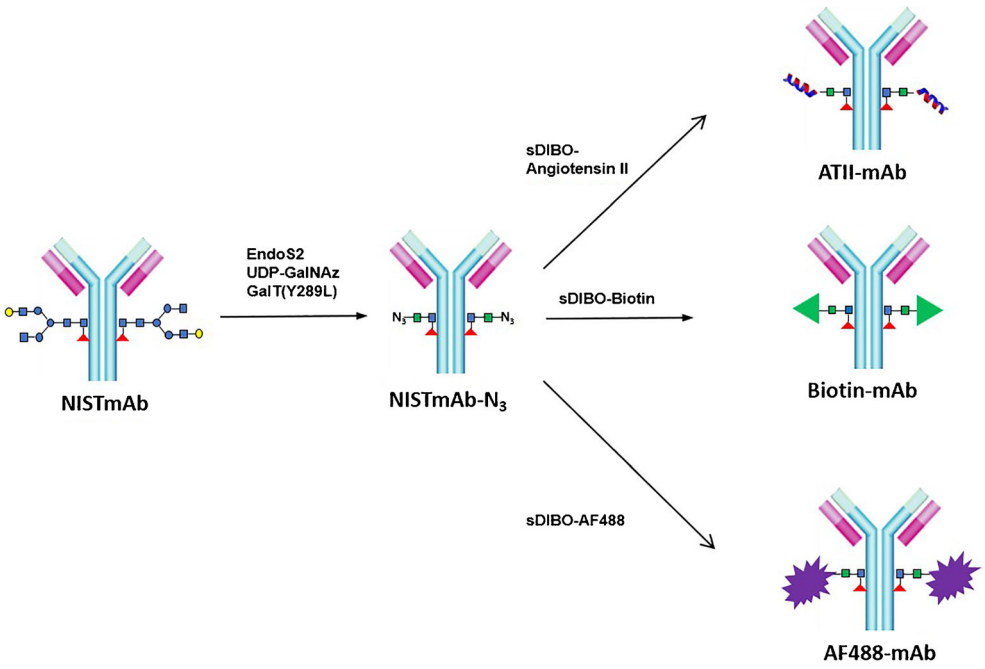

Fig. 1 Reaction scheme used for preparation of NISTmAb antibody drug conjugate mimetics (note the green square shown bound to N_3 represents GalNAz, while the blue square bound to fucose (red triangle) represents GlcNAc)

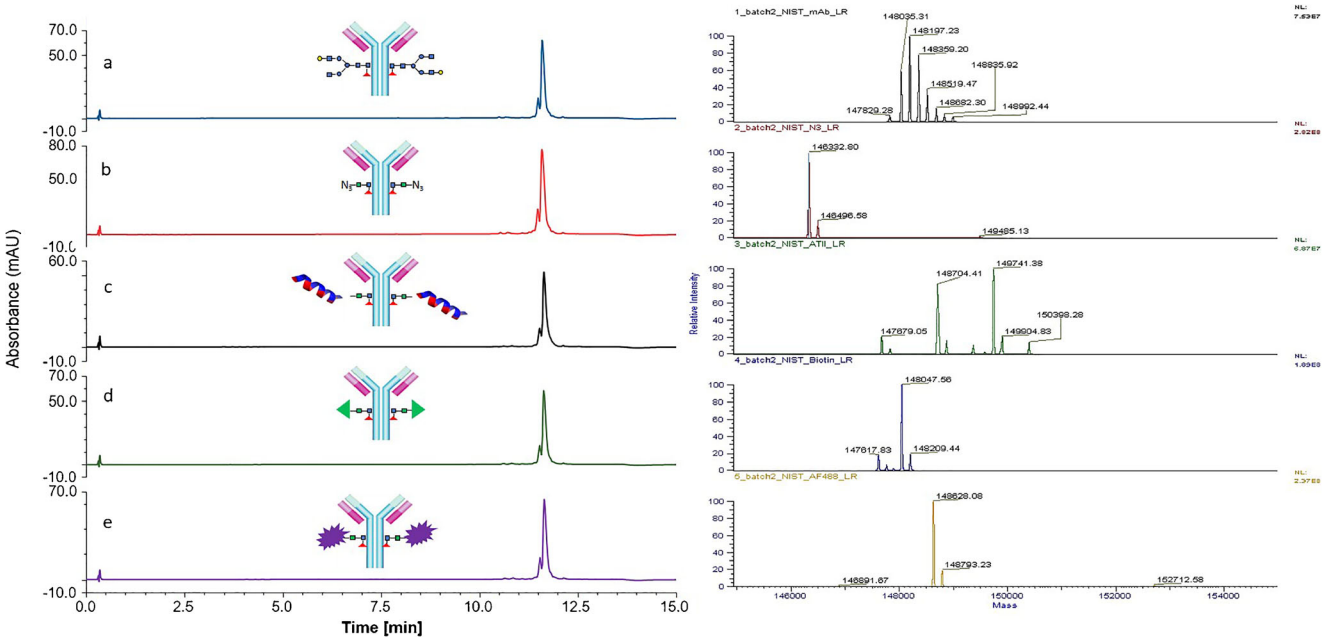

Fig. 2 LC-UV (left) and LC-MS (right) analyses of NISTmAb (a), azide-activated NISTmAb (b), ATII-mAb (c), Biotin-mAb (d), and AF488-mAb (e)

functional groups. Similarly, intact LC-MS analysis of the final ADC conjugates (Fig. 2c–e) indicates the presence of the desired ATII-mAb, Biotin-mAb, and AF488-mAb structures with masses confirmed to within 15 ppm (ESM Table S2). Two additional minor peaks were identified in the ATII-mAb spectrum which were determined to be products of an sDIBO synthetic intermediate impurity (sDIBO-acid) formed during the synthesis of the sDIBO-ATII intermediate compound. The peaks are shown in the right panel of Fig. 2c (ATII-mAb). The 148,704.41 peak represents a species with one sDIBO-ATII and one sDIBO-acid, and the peak at 147,679.05 represents the species with two sDIBO-acids (further discussion below). While these masses had a slightly larger error than other identified species, orthogonal mass spectrometry approaches discussed below support these assignments. Similarly, one additional minor peak was identified in the Biotin-mAb spectrum which was determined to be the product of an sDIBO synthetic intermediate impurity (sDIBO-acid) formed during the synthesis of the sDIBO-Biotin intermediated compound. The peak is shown in Fig. 2d, right panel (Biotin-mAb). The 147,617.83 peak represents a species with one sDIBO-Biotin and one sDIBO-acid. Further characterizations of these minor species are discussed below.

Middle-down mass spectrometry Middle-down MS utilized an enzyme called IdeS to selectively cleave the hinge region of NISTmAb between the two conserved G-G residues. The result is the production of a 100-kD $F(ab)_2$ antigen binding domain and two 25-kD scFc domains. Reduction of the $F(ab)_2$ disulfide bonds is often performed to produce the constituent light-chain (LC) and heavy-chain fragments (both ≈ 25 kDa) to take advantage of additional mass resolving power at lower *m/z* range. The chemoenzymatic conjugation strategy selected is particularly suited for middle-down MS without reduction of the $F(ab)_2$ because the NISTmAb glycan-targeted conjugation site is located on the scFc domain. This workflow takes full advantage of the subunit selectivity following EndoS2 cleavage as well as the improved mass resolution by directly measuring the 25-kDa scFc, while minimizing offline sample preparation (e.g., no need for reduction) that may induce unwanted chemical modifications into the analysis. LC-UV and LC-MS analyses for the non-reduced middle-down analysis of the NISTmAb, NISTmAb-N_3 intermediate, and each of the ADC mimics are shown in Fig. 3. The chromatographic retention behavior and the observed masses for the $F(ab)_2$ fragments are shown to have identical elution times and structure. This is consistent with the conjugation site occurring specifically on the Fc domain.

The scFc elutes as a single well-behaved peak in the LC-UV and LC-MS method following EndoS2 glycan cleavage and GalNAz functionalization. The EndoS2 and GalT(Y289L) synthesis steps are highly efficient, with near complete conversion of the glycosylated scFc masses into the desired GalNAz functionalized species, verified via the accurate mass measurements as listed in ESM Table S3. Continued synthetic steps were also highly efficient, resulting in the expected conjugated species as indicated by the observed masses in ESM Table S3. As mentioned above, we identified additional minor peaks in the ATII-mAb mass spectrum that are confirmed to be the result of a synthetic intermediate impurity formed during the synthesis of the sDIBO-compound. As such, we identified an additional peak in the middle down analysis that

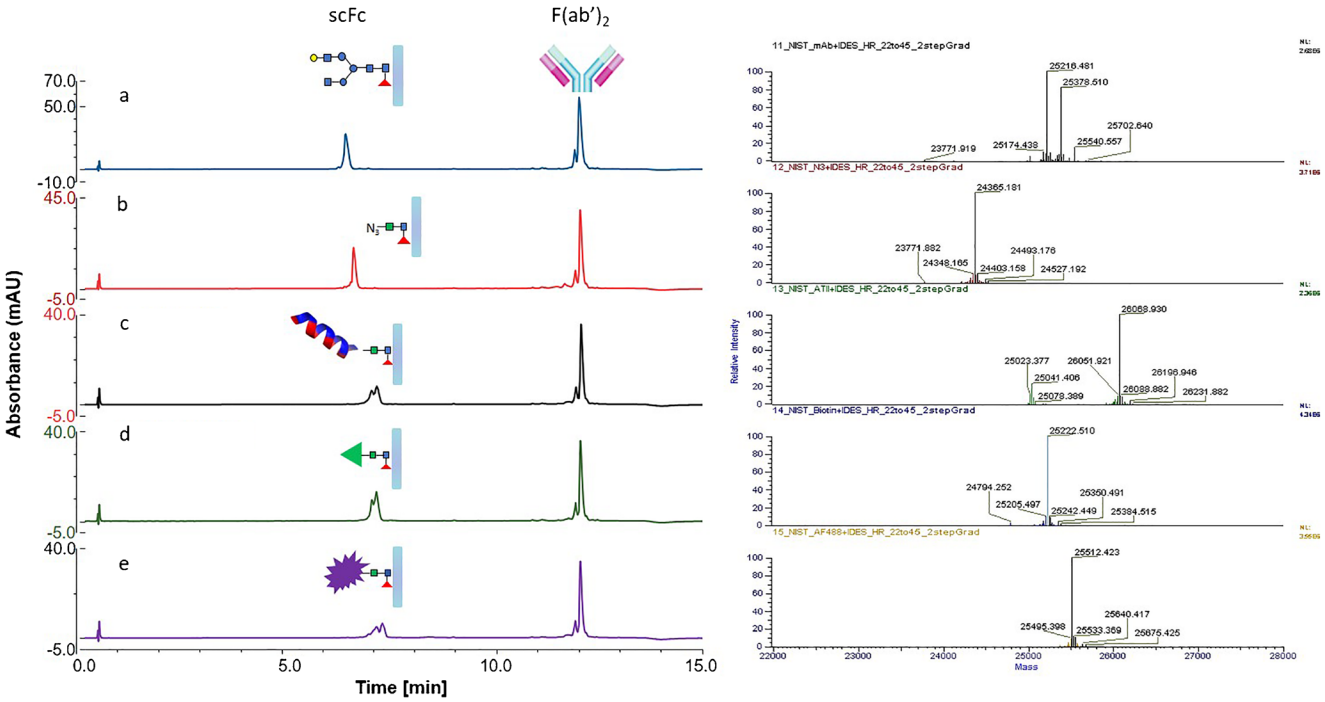

Fig. 3 LC-UV (left) and deconvoluted LC-MS of the scFc (right) analyses of IdeS-treated NISTmAb (a), azide-activated NISTmAb (b), ATII-mAb (c), Biotin-mAb (d), and AF488-mAb (e)

represents the addition of a single compound identified as the sDIBO-acid which was a minor product derived from the hydrolysis of the sDIBO-SDP reagent utilized in the synthesis of the sDIBO-ATII reagent. In the middle-down analysis (Fig. 3c), only a single peak (25,041.406) was identified (versus 2 in the intact analysis above), as the heavy chains of the Fc domain are dissociated, and therefore only the ATII or the acid-containing species are identified, not the combination as in the intact analysis above. This was not surprising as the sDIBO-ATII peptide was purified by a single HPLC run and was not completely separated from the side-reaction species in a single column pass. A similar but much smaller peak (24,794.252) in the Biotin-mAb spectrum (Fig. 3d) is similarly the result of an sDIBO-acid synthetic intermediate of the sDIBO-Biotin compound.

It is also worth noting that the scFc fragments for each of the conjugates elute in the LC-UV methods as unresolved split peaks (Fig. 3a–e), yet the identified masses are consistent with the expected sDIBO-conjugated species throughout the entirety of the peaks. This split peak behavior is attributed to the formation of structural isomers resulting from the triazolyl ring formation of the sDIBO copperless click reaction, a non-regioselective process, discussed in more detail below in the peptide mapping section.

Peptide mapping LC-MS/MS peptide mapping was carried out as an extended characterization assay to further validate intact and middle-down mass spectrometry results. Figure S1 (see ESM) depicts a comparison of the total ion chromatogram (TIC) results for RM 8671 and the final Alexa Fluor 488 conjugate as a representative example. Visual inspection of the two chromatograms demonstrates a conformation to expectation for most peaks, disappearance of the glycopeptide peaks, and a new series of peaks are observed eluting between 25 and 30 min. Similar results were obtained for all conjugates, with all peaks conforming to expectation with the exception of new peaks arising from the pertinent conjugations at the heavy-chain Asn 300 glycosylation site peptide (EEQYnSTYR).

Glycosylation of RM 8671, as well as the new peaks observed in the conjugate chromatograms, was verified via LC-MS/MS spectral matching as described in the "Materials and methods" section. High mass accuracy MS1 (within 10 ppm) and MS/MS fragmentation consistent with the putative identity of each peptide were required to confidently match parent ions to conjugate peptides. A representative MS/MS spectrum of the triply charged AF488 conjugate peptide is shown in Fig. S2 (see ESM). Biotin-mAb and ATII-mAb conjugate peptides showed similar patterns dominated by glycosidic linkage fragmentation in the conjugate side chain, confidently verifying selective conjugation at Asn 300 of the heavy chain. Confirmed species are listed in ESM Table S4 for the dominant EEQYnSTYR glycopeptide along with relative abundance values calculated based on extracted ion chromatograms (XICs). RM 8671 was observed to contain

predominantly complex biantennary fucosylated glycans as well as low abundance high mannose, afucosylated, and aglycosylated species. The desired synthetic intermediates of the EndoS2-cleaved and NISTmAb-N_3 samples were achieved with complete conversion to the requisite fucosylated and non-fucosylated N-glycoconjugates. The final ADC mimetics showed similarly good yield; quantitative analysis based on XICs showed that the desired predominant products, a conjugated glycopeptide containing the original GlcNAc-Fuc (N1F1) or GlcNAc (N) core, dominates at 80.8 to 98.1% relative abundance in each case. Consistent with the results from the intact and middle-down analyses, an additional modified EEQYnSTYR peptide was identified by peptide mapping that represents the sDIBO-acid conjugated synthetic by-product in both the ATII-mAb and Biotin-mAb samples. These synthetic impurities were each identified at a shifted retention time from the desired conjugate product, indicating the origin of the impurity was not due to in-source decay in the intact or middle-down results (data not shown). Quantitation of these sDIBO-acid peptide products resulted in approximately 19.0% and 2.7% relative abundance for the ATII and biotin compounds, respectively (ESM Table S4). Further purification of the sDIBO-precursor starting materials would yield > 99% of the desired ADC mimetic products.

A small quantity of aglycosylated peptide was observed in each of the samples, remaining relatively consistent throughout the synthesis steps (ESM Table S4). In addition, the conjugated peptide containing an afucosylated core was also observed in each synthesis step as well as in the final products. This is not unexpected considering the NISTmAb is known to have low levels of afucosylated glycans. A slight increase in afucosylated conjugates in the synthesis intermediates as well as final products (vs. RM 8671) was observed. This increase is thought to be predominantly due to in-source fragmentation as fucosyl and afucosyl species co-eluted in each case, with the degree of co-elution being greatest for the NISTmAbES2 (the species generated by EndoS cleavage) and NISTmAb-N_3 samples.

Peptide mapping also provided more in-depth selectivity for characterization of the final glycoconjugate. As demonstrated in Fig. 4, a series of new relatively high abundance peaks were observed in the final glycoconjugate products as opposed to a single high abundance peak. To evaluate this further, extracted ion chromatograms were prepared for the 3+ charge state of the expected final glycoconjugate peptides in each sample (Fig. 4). The XICs clearly show single peaks for the G0F NISTmAb glycopeptide as well as for the NISTmAb-ES2 and NISTmAb-N_3 synthesis intermediates. In each of the final glycoconjugate samples, however, a series of 7–8 isomeric peaks is observed, each of which corresponds to the same expected parent mass and MS/MS spectrum of the desired end-product glycoconjugate. These isomers are the likely result of the synthetic strategy utilized for the initial mimetic materials since the sDIBO cycloaddition is not regioselective, and isometrically pure starting reagents were not utilized. The final products contained a total of three stereogenic centers, therefore explaining the presence of eight isomers eluting at different retention times for ATII-mAb. In the case of Biotin-mAb and AF488-mAb where only seven isomer peaks are observed, it is possible that an eighth isomer is obscured by co-elution.

Lastly, peptide mapping affords the opportunity to identify post-translational modifications as well as potential changes in chemical modifications as a result of chemical synthesis steps. A series of residues were identified with low levels of asparagine deamidation and methionine oxidation in the RM 8671 starting material (ESM Table S5), consistent with previous results [32]. Each of these modifications was also observed in the synthesis intermediates as well as the final glycoconjugate products. Figure 5 depicts the summed deamidation (Fig. 5a) and summed oxidation (Fig. 5b) for each of the individual samples, with site-specific values listed in ESM Table S5. Deamidation was relatively consistent throughout the synthesis procedures, with summed deamidation of approximately 8.5% relative abundance, indicating synthesis conditions have minimal effect on deamidation. Oxidation, on the other hand, was shown to increase slightly with each synthesis step. The increase in oxidation was rather small, however, and additional process replicates would be required to validate the magnitude and consistency of the observed change.

Discussion

The challenges in elucidation of structure for antibody drug conjugate products are magnified relative to standalone monoclonal antibody products. The addition of a toxin payload greatly increases the complexity of the drug, especially if randomly conjugated, and therefore comprehensive characterization is necessary to ensure the purity, stability, safety, and efficacy of that material for its intended purpose. Following conjugation, the material must undergo a second round of rigorous analytical characterization to validate efficient and consistent conjugation as well as to ensure the mAb construct maintains its form and function. The extended synthetic processing, which in some cases may expose the mAb to reducing, oxidizing, or other harsh conditions, makes extended characterization of ADCs an absolutely critical component of their development.

Adaptation of technologies from mAb therapeutics, as well as innovation of ADC-specific characterization technologies, has thus far been performed using manufacturer-specific materials and/or small-scale mimetic synthesis. These examples have provided an infrastructure for further development; however, industry-wide method evaluation and advancement

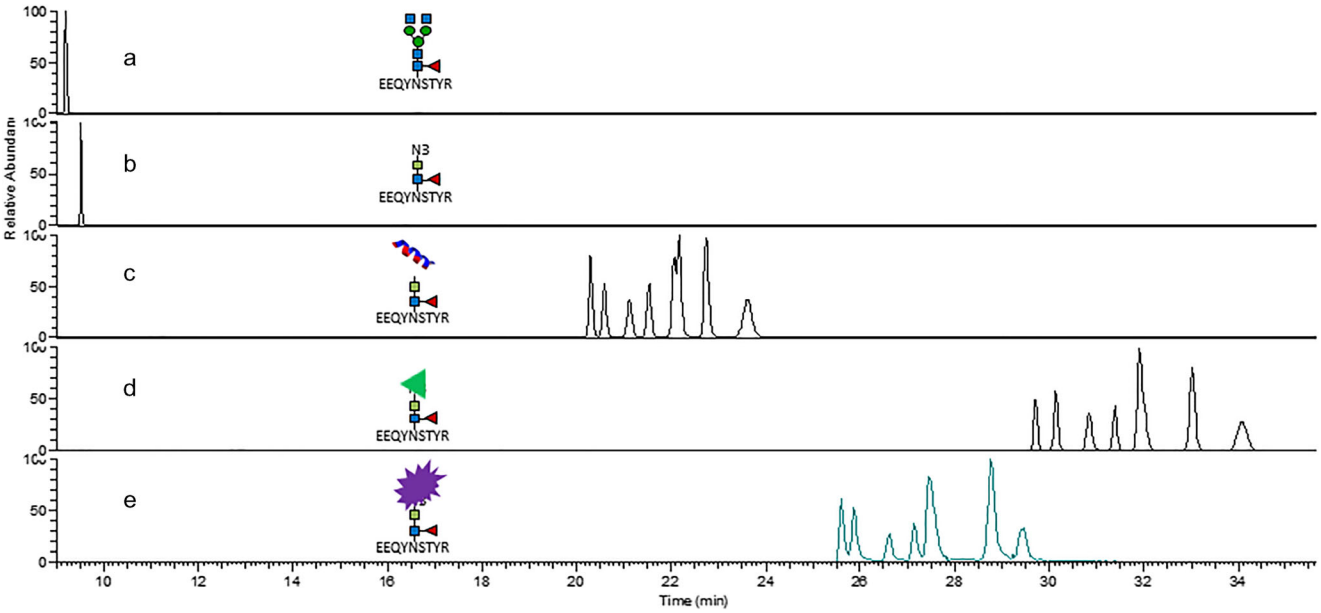

Fig. 4 Extracted ion chromatograms (15 ppm) for the glycoconjugate peptide monoisotopic $[M+3H]^{3+}$ ion of (a) G0F glycan in NISTmAb sample, (b) GalNAz conjugate in NISTmAb-N_3 sample, (c) Angiotensin II conjugate in ATII-mAb sample, (d) biotin conjugate in Biotin-mAb sample, and (e) Alexa Fluor 488 conjugate in AF488-mAb sample

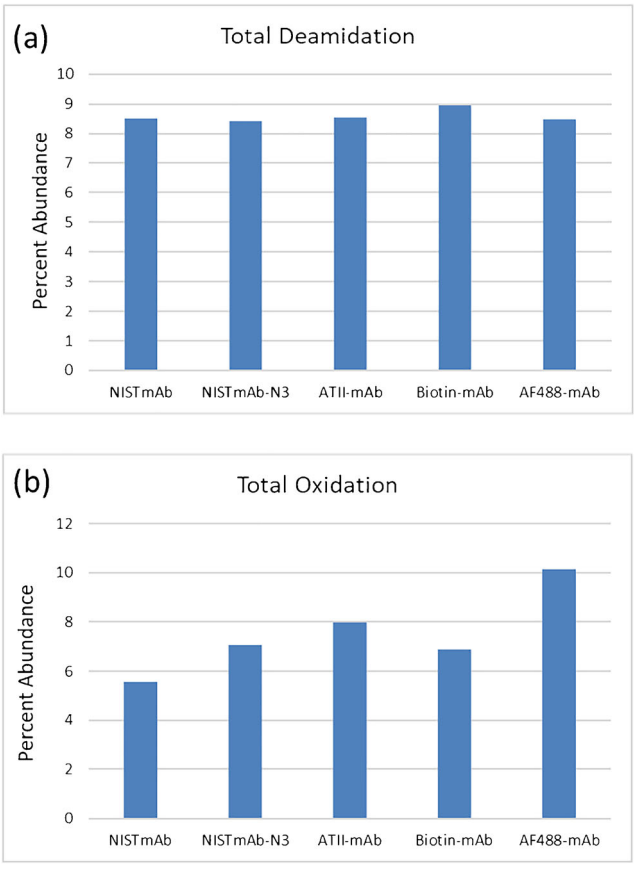

Fig. 5 Summed relative abundance of post-translational modifications observed for glycoconjugate materials. Table S4 in ESM contains site-specific data

would benefit from the use of common, pre-competitive materials. A variety of product-specific complexities exist with ADCs (IgG class, attachment site, linker chemistry, etc.), which in turn may require multiple materials to fully cover the product-specific complexities of this class. On the other hand, many analytical approaches are shared between classes of ADCs, including the extended mass spectrometry-based approaches applied herein. A small subset of materials, or even well-defined protocols for their synthesis, may fulfill the need for ADC representative analytical test metrics, the first of which is described here.

Here, we applied a series of advanced mass spectrometry-based techniques to fully characterize the ADC mimetic conjugates. To summarize, the primary deglycosylation step utilizing EndoS2 enzyme to generate core fucosylated (or non-fucosylated) GlcNAc residues was completely efficient in that no glycan-containing peptides were identified in peptide mapping experiments. Secondly, after chemoenzymatic activation with GalNAz, none of the antibody species was identified that contained unmodified core GlcNAc residues by any of the methods used. Lastly, after chemical conjugation with sDIBO, no antibody species were identified that contained free GalNAz-containing residues.

The NISTmAb RM 8671 was selected as the industry representative mAb for initial ADC mimic proof-of-principle. The NISTmAb shares the IgG1 subclass with many of the approved ADC therapeutics and also provides a highly characterized starting material whose historical characterization dataset can be leveraged. Design features of an industry-relevant ADC standard beyond the NISTmAb framework, however, become increasingly complicated by the sheer

breadth of variations in conjugation methods and linker chemistries either undergoing clinical testing or approved by the FDA. As the NISTmAb does not contain any pre-engineered free cysteines or biorthogonal reactive moieties, we chose to modify the antibody using chemoenzymatic engineering of the naturally occurring heavy-chain glycans to prepare homogenously conjugated NISTmAb ADC mimetics with DAR = 2.0. As mentioned above, one advantage of this labeling approach is that it does not require any genetic modification or recombinant expression of the antibody and therefore allows the development of ADC constructs with essentially any pre-existing antibody.

The ideal payload for an ADC mimetic would be of similar size and composition as a payload used for a therapeutic ADC, except it would be non-toxic to allow more widespread utility in both academic, vendor, and industrial labs. Angiotensin II was selected as the peptide mimetic payload due to its widespread use in analytical laboratories and the presence of a tryptic cleavage site to model potential analytical challenges. Biotin and Alexa Fluor 488 were also used as small molecule mimics as they are non-toxic and cost-effective, and are reasonably similar in mass to therapeutic payloads. These molecules were also selected due to their unique properties, with biotin being a common affinity purification/detection ligand and Alexa Fluor 488 known for its stability and high fluorescence yield.

High mass accuracy mass spectrometry-based characterization was utilized to monitor synthetic fidelity as well as the final product quality of the NISTmAb ADC glycoconjugates. Intact mass spectrometry was demonstrated as a high-throughput method capable of monitoring each synthetic step as well as final product characterization. Middle-down analysis of the NISTmAb mimetics also demonstrated very high synthetic yield. The dominant products identified were the expected conjugates with only minor sub-species identified. Non-reduced middle-down analyses provide benefit in terms of both chromatographic selectivity and mass resolution. The high mass accuracy in both cases provides confident assignment of the ADC conjugates and evaluation of the number of payloads per molecule.

A measure of DAR can be made using intact mass spectrometry and the related method SEC-MS. Deglycosylation with PNGase F is often used prior to mass analysis in an effort to minimize heterogeneity associated with Fc glycans and simplify DAR determination. Accurate mass identification of products differing in the number of payloads per molecule is used with associated area under the curve analysis of the resulting deconvoluted mass spectra to provide a measure of average DAR. In the current ADC synthesis strategy, the Endo S treatment is a deglycosylation step, enabling direct DAR calculation (intact MS) or drug to polypeptide (DPP) calculation (middle down and peptide mapping) using the final product in each method. It is important to note that reaction yield and DAR/DPP are quite different metrics in the case of glycan conjugation. Aglycosylated species are not available for reaction, for example, but affect the final DAR of the product. Similarly, the small molecule sDIBO-acid molecules represent chemical fidelity of the reaction, but are impurities in the final product and are thus not considered as part of the desired conjugate in a DAR calculation.

Deconvolution of the intact antibody drug conjugate mimics listed in ESM Table S2 can yield relative abundance values for desired conjugates containing two payloads (DAR = 2), sDIBO acid species containing one payload and one sDIBO acid (DAR = 1), and species containing two sDIBO acid intermediates. Each of these species may also be identified as different proteoforms representing normal mAb heterogeneity (i.e., glycation, C-terminal lysine, etc.). DAR was therefore calculated as DAR = (2*%RA DAR2-mAb + %RA DAR1-mAb)/100, yielding values of 1.46, 1.87, and 2 for the ATII, Biotin, and AF488 species, respectively.

High-resolution MS analysis of the scFc fragments and peptide map data for ATII-mAb, Biotin-mAb, and AF488-mAb showed similar results as the intact analysis with regard to species identified. With regard to payload conjugation, it is important to note that middle-down mass spectrometry and peptide mapping technically report a drug to scFc and drug to peptide ratio, which we will refer to as the drug to polypeptide ratio (DPP). Middle-down analysis yielded DPP of 1.63, 1.93, and 2 for ATII-mAb, Biotin-mAb, and AF488-mAb (DPP = 2* %RA conjugated polypeptide-proteoform/100). Peptide mapping analysis yielded DPP of 1.62, 2.00, and 1.99 for ATII-mAb, Biotin-mAb, and AF488-mAb (DPP = 2* %RA conjugated polypeptide-proteoform/100).

The ATII data is useful to exemplify the different interpretation of DAR vs. DPP (calculated from the bottom up peptide mapping), wherein DAR < DPP in each case. Measurement of the conjugated scFc and peptide does not allow for the presence of the mixed species (one sDIBO acid and one proper conjugate) to be considered in the calculation. Importantly, however, the ability to detect low abundance proteoforms is known to be improved in middle-down and peptide mapping (e.g., the afucosylated species in the current dataset) and yields a more comprehensive characterization. A variety of additional LC-based methods (e.g., hydrophobic interaction liquid chromatography, among others) may also be utilized to calculate DAR. Numerous factors can contribute to disparity between DAR values calculated by different methods, some of which are highlighted by the current data. While the current dataset provides a limited comparison of individual methods, it does serve as a benchmark for future interlaboratory studies to delve deeper into sources of uncertainty and bias that may result as a function of method selected and highlights the need for reporting DAR or DPP calculation method.

The NISTmAb ADC conjugate DAR determination serves as an example as to the utility of these materials for ADC-

specific measurement innovation and harmonization. The materials were specifically designed with a DAR = 2 target in mind to most closely represent this desired feature of next-generation ADCs. DAR is the most widespread and highly discussed analytical measure and is applied to each and every ADC and numerous analytical methods and data treatment software exist for its determination. The ADC mimetics produced herein afford a broader cross-industry comparison platform for DAR determination methods. The use of a nearly quantitative DAR = 2 material affords a relatively simple material (compared to non-site-specific DAR > 2 material) to begin to identify inter-method variations, interlaboratory variations, and the underlying method-specific principles that may lead to those variations.

Highly sensitive mass analyses allowed for the identification of low abundance synthetic intermediates for both ATII-mAb and Biotin-mAb. As such, these ADC mimetics serve to provide a real-life situation whereby small amounts of synthetic contaminants can be readily identified and characterized. The current dataset also exemplifies that DAR alone does not structurally describe the full molecular properties of an ADC; conjugation site, site occupancy, and potential conjugation-induced heterogeneities also exist. Peptide mapping was utilized as an extended characterization strategy to exhaustively verify the site-specific conjugation. Peptide mapping confirmed that each synthetic step provided a near quantitative yield of conjugated product; in each case, the desired FucoseGlcNAc-glycoconjugate was the major tryptic peptide. A small portion of aglycosylated species was consistent in each sample as expected, but none of the glycoforms observed in RM 8671 was observed in the peptide map of synthetic process intermediates or the final products. The increased sensitivity of peptide mapping vs. intact/middle down also afforded identification of the afucosylated N-glycoconjugate. The NISTmAb has been previously shown to contain low levels of afucosylated glycan, and therefore observation of this species is expected, and serves as an indication of the utility of the peptide map with regard to comprehensive conjugate identification. The final glycoconjugate peptides were revealed to consist of a series of isomers identifiable only via chromatographic resolution during peptide mapping and all corresponded to the same expected parent mass and MS/MS spectrum of the desired end-product glycoconjugates. Collectively, the site-specific conjugation yield was determined to be > 99% based on the sum of fucosylated and afucosylated core-GlcNAc conjugates.

LC-MS/MS peptide mapping also increased characterization depth via low abundance PTM identification and quantification. LC-MS/MS demonstrated that the NISTmAb was relatively resistant to chemical modification throughout the entire conjugation procedure. Deamidation was consistent in all products, although a minor increase in oxidation was observed. As such, the optimization of pH conditions, dialysis times, and careful exclusion of oxidative conditions during the conjugation workflow may reduce even further the small amount of oxidation observed here. Evaluation of additional future batches and/or scale-up efforts will allow determination of process consistency with regard to these chemical modifications; therefore, continued process development will greatly benefit from the quantitative capabilities of the developed LC-MS method. The specific type and location of aberrant PTMs in ADCs, such as oxidation and deamidation, are important during process development because they can affect safety, efficacy, and stability of mAb-based therapeutics

The LC-MS/MS method herein provides a seamless transition toward attribute-specific control strategies and impurity detection as is currently implemented in multi-attribute method (MAM) mass spectrometry. MAM applied to ADCs would allow quantitative monitoring of synthetic yield at critical conjugation steps and most importantly inform on site-specific conjugation fidelity and consistency. ADCs are a prime therapeutic modality for implementation of MAM due to the high criticality and potential implications of conjugation site occupancy. The ADC glycoconjugates described herein provide a means for de-risking and exemplifying MAM-based analysis on a pre-competitive ADC material. Extended characterization of the ADC glycoconjugate mimics revealed subtle heterogeneities including those that are intrinsic to the conjugation chemistry used (e.g., cycloaddition regioselectivity and payload isomerism), intrinsic mAb glycan heterogeneity, conjugation product impurities, and those that are intrinsic to the mAb (e.g., PTMs). Heterogeneity is expected in any ADC and exemplifies the need for high process understanding and deep product characterization. Extended characterization of ADCs does not stop here, however, and the use of numerous innovative technologies such as those for higher order structure (NMR, HDX, etc.) is likely to increase. Pre-competitive reference materials would allow a systematic evaluation and comparison of novel technologies by removing product-to-product heterogeneity from analytical method figures of merit. In turn, a common test metric will provide expedited uptake of the specific technologies that will most efficiently and effectively impact product development.

Conclusions

We have used here a highly efficient chemoenzymatic glycoconjugation method to generate three glycoconjugate ADC mimetics with differing payloads to represent both small molecule and peptide conjugated ADCs. Remarkably, the 2-step conjugation process was essentially 99% efficient resulting in the production of three highly homogenous non-toxic ADC analogues. A series of mass spectrometry-based characterization tools were performed on each of the mimetics to evaluate synthetic fidelity as well as product quality

attributes. Aberrant low-abundance product species were identified and characterized, and were found to result from raw material contaminants present during the sDIBO-linker synthesis. The NISTmAb ADC mimetics represent novel analytical materials and the associated preparation/characterization strategy may serve as a guideline for development of related protocols/materials with orthogonal properties. The resulting materials herein as well as those prepared in a similar strategy may provide analytical challenge materials suitable for method development, evolution, and control.

The fact that the chemoenzymatic method used here allows for the preparation of ADCs without the requirement for a site-specific genetically engineered platform enables a broad spectrum of researchers to prepare site-specifically conjugated ADCs who otherwise would not have the capability or resources to do so. Finally, the non-toxic well-characterized payloads utilized here are known to be benign, are stable, and therefore may prove to be beneficial for expanded studies beyond the scope of this paper, but nonetheless are within the realm of commonly used cell biological ADC evaluation techniques. The constructs can be used to characterize ADC-linker properties including in vitro and in vivo cleavability and stability. Other potential applications may include use in vitro and in vivo biological membrane transport studies, and quantitative pull-down studies. Although each of the three constructs carries different payloads, the DARs and specific attachment sites are identical, and therefore a significant level of variability is removed when applied to concomitant cell biological studies.

Supplementary Information The online version contains supplementary material available at https://doi.org/10.1007/s00216-021-03460-y.

Declarations

Conflict of interest The authors declare no competing interests.

References

1. Mouchahoir T, Schiel JE. Development of an LC-MS/MS peptide mapping protocol for the NISTmAb. Anal Bioanal Chem. 2018;410(8):2111–26. https://doi.org/10.1007/s00216-018-0848-6.
2. Schiel JE, Turner A. The NISTmAb Reference Material 8671 lifecycle management and quality plan. Anal Bioanal Chem. 2018;410(8):2067–78. https://doi.org/10.1007/s00216-017-0844-2.
3. Schiel JE, Turner A, Mouchahoir T, Yandrofski K, Telikepalli S, King J, et al. The NISTmAb Reference Material 8671 value assignment, homogeneity, and stability. Anal Bioanal Chem. 2018;410(8):2127–39. https://doi.org/10.1007/s00216-017-0800-1.
4. Turner A, Schiel JE. Qualification of NISTmAb charge heterogeneity control assays. Anal Bioanal Chem. 2018;410(8):2079–93. https://doi.org/10.1007/s00216-017-0816-6.
5. Turner A, Yandrofski K, Telikepalli S, King J, Heckert A, Filliben J, et al. Development of orthogonal NISTmAb size heterogeneity control methods. Anal Bioanal Chem. 2018;410(8):2095–110. https://doi.org/10.1007/s00216-017-0819-3.
6. Arbogast LW, Delaglio F, Schiel JE, Marino JP. Multivariate Analysis of Two-Dimensional (1)H, (13)C Methyl NMR spectra of monoclonal antibody therapeutics to facilitate assessment of higher order structure. Anal Chem. 2017;89(21):11839–45. https://doi.org/10.1021/acs.analchem.7b03571.
7. Brinson RG, Marino JP, Delaglio F, Arbogast LW, Evans RM, Kearsley A, et al. Enabling adoption of 2D-NMR for the higher order structure assessment of monoclonal antibody therapeutics. mAbs. 2018. https://doi.org/10.1080/19420862.2018.1544454.
8. Castellanos MM, Howell SC, Gallagher DT, Curtis JE. Characterization of the NISTmAb Reference Material using small-angle scattering and molecular simulation : part I: dilute protein solutions. Anal Bioanal Chem. 2018. https://doi.org/10.1007/s00216-018-0868-2.
9. Castellanos MM, Mattison K, Krueger S, Curtis JE. Characterization of the NISTmAb Reference Material using small-angle scattering and molecular simulation : part II: concentrated protein solutions. Anal Bioanal Chem. 2018. https://doi.org/10.1007/s00216-018-0869-1.
10. Cavicchi RE, King J, Ripple DC. Measurement of average aggregate density by sedimentation and Brownian motion analysis. J Pharm Sci. 2018;107(5):1304–12. https://doi.org/10.1016/j.xphs.2018.01.013.
11. Dong Q, Liang Y, Yan X, Markey SP, Mirokhin YA, Tchekhovskoi DV, et al. The NISTmAb tryptic peptide spectral library for monoclonal antibody characterization. mAbs. 2018;10(3):354–69. https://doi.org/10.1080/19420862.2018.1436921.
12. Dong Q, Yan X, Liang Y, Stein SE. In-depth characterization and spectral library building of glycopeptides in the tryptic digest of a monoclonal antibody using 1D and 2D LC-MS/MS. J Proteome Res. 2016;15(5):1472–86. https://doi.org/10.1021/acs.jproteome.5b01046.
13. Gallagher DT, Karageorgos I, Hudgens JW, Galvin CV. Data on crystal organization in the structure of the Fab fragment from the NIST reference antibody, RM 8671. Data in brief. 2018;16:29–36. https://doi.org/10.1016/j.dib.2017.11.013.
14. Hill JJ, Tremblay TL, Corbeil CR, Purisima EO, Sulea T. An accurate TMT-based approach to quantify and model lysine susceptibility to conjugation via N-hydroxysuccinimide esters in a monoclonal antibody. Sci Rep. 2018;8(1):17680. https://doi.org/10.1038/s41598-018-35924-0.
15. Hilliard M, Alley WR Jr, McManus CA, Yu YQ, Hallinan S, Gebler J, et al. Glycan characterization of the NIST RM monoclonal antibody using a total analytical solution: from sample preparation to data analysis. mAbs. 2017;9(8):1349–59. https://doi.org/10.1080/19420862.2017.1377381.
16. Kalonia CK, Heinrich F, Curtis JE, Raman S, Miller MA, Hudson SD. Protein adsorption and layer formation at the stainless steel-solution interface mediates shear-induced particle formation for an IgG1 monoclonal antibody. Mol Pharm. 2018;15(3):1319–31. https://doi.org/10.1021/acs.molpharmaceut.7b01127.
17. Karageorgos I, Gallagher ES, Galvin C, Gallagher DT, Hudgens JW. Biophysical characterization and structure of the Fab fragment from the NIST reference antibody, RM 8671. Biologicals. 2017;50:27–34. https://doi.org/10.1016/j.biologicals.2017.09.005.
18. Schiel JE, Davis DL, Borisov OB (eds) (2015) State-of-the-art and emerging technologies for therapeutic monoclonal antibody characterization volume 3. Defining the next generation of analytical and biophysical techniques, vol 1202. ACS Symposium Series, vol 1202. American Chemical Society. doi:https://doi.org/10.1021/bk-2015-1202
19. Schiel JE, Davis DL, Borisov OB (eds) (2015) State-of-the-art and emerging technologies for therapeutic monoclonal antibody

characterization volume 2. Biopharmaceutical Characterization: The NISTmAb Case Study, vol 1201. ACS Symposium Series, vol 1201. American Chemical Society. doi:https://doi.org/10.1021/bk-2015-1201

20. van der Burgt YEM, Kilgour DPA, Tsybin YO, Srzentic K, Fornelli L, Beck A, et al. Structural analysis of monoclonal antibodies by ultra-high resolution MALDI In-Source Decay FT-ICR mass spectrometry. Anal Chem. 2018. https://doi.org/10.1021/acs.analchem.8b04515.
21. Singh SK, Luisi DL, Pak RH. Antibody-drug conjugates: design, formulation and physicochemical stability. Pharm Res. 2015;32(11):3541–71. https://doi.org/10.1007/s11095-015-1704-4.
22. Rathore D, Faustino A, Schiel J, Pang E, Boyne M, Rogstad S. The role of mass spectrometry in the characterization of biologic protein products. Expert Rev Proteomics. 2018;15(5):431–49. https://doi.org/10.1080/14789450.2018.1469982.
23. Jain N, Smith SW, Ghone S, Tomczuk B. Current ADC linker chemistry. Pharm Res. 2015;32(11):3526–40. https://doi.org/10.1007/s11095-015-1657-7.
24. Ponziani S, Di Vittorio G, Pitari G, Cimini AM, Ardini M, Gentile R, et al. Antibody-drug conjugates: the new frontier of chemotherapy. Intl. J Pharm Sci. 2020;21(15). https://doi.org/10.3390/ijms21155510.
25. Sadiki A, Vaidya SR, Abdollahi M, Bhardwaj G, Dolan ME, Turna H, et al. Site-specific conjugation of native antibody. Antibody therapeutics. 2020;3(4):271–84. https://doi.org/10.1093/abt/tbaa027.
26. Valliere-Douglass JF, McFee WA, Salas-Solano O. Native intact mass determination of antibodies conjugated with monomethyl Auristatin E and F at interchain cysteine residues. Anal Chem. 2012;84(6):2843–9. https://doi.org/10.1021/ac203346c.
27. Beckley NS, Lazzareschi KP, Chih HW, Sharma VK, Flores HL. Investigation into temperature-induced aggregation of an antibody drug conjugate. Bioconjug Chem. 2013;24(10):1674–83. https://doi.org/10.1021/bc400182x.
28. Guo J, Kumar S, Prashad A, Starkey J, Singh SK. Assessment of physical stability of an antibody drug conjugate by higher order structure analysis: impact of thiol- maleimide chemistry. Pharm Res. 2014;31(7):1710–23. https://doi.org/10.1007/s11095-013-1274-2.
29. Prien JM, Stöckmann H, Albrecht S, Martin SM, Varatta M, Furtado M, Hosselet S, Wang M, Formolo T, Rudd PM, Schiel JE Orthogonal technologies for NISTmAb N-glycan structure elucidation and quantitation. In: State-of-the-art and emerging technologies for therapeutic monoclonal antibody characterization volume 2. Biopharmaceutical Characterization: The NISTmAb Case Study, vol 1201. ACS Symposium Series, vol 1201. American Chemical Society. 2015; pp 185-235. doi:https://doi.org/10.1021/bk-2015-1201.ch004
30. Sjögren J, Cosgrave EF, Allhorn M, Nordgren M, Björk S, Olsson F, et al. EndoS and EndoS2 hydrolyze Fc-glycans on therapeutic antibodies with different glycoform selectivity and can be used for rapid quantification of high-mannose glycans. Glycobiology. 2015;25(10):1053–63. https://doi.org/10.1093/glycob/cwv047.
31. Qasba PK. Glycans of antibodies as a specific site for drug conjugation using glycosyltransferases. Bioconjug Chem. 2015;26(11):2170–5. https://doi.org/10.1021/acs.bioconjchem.5b00173.
32. Li W, Kerwin JL, Schiel J, Formolo T, Davis D, Mahan A, Benchaar SA. Structural elucidation of post-translational modifications in monoclonal antibodies. In: State-of-the-art and emerging technologies for therapeutic monoclonal antibody characterization volume 2. Biopharmaceutical Characterization: The NISTmAb Case Study, vol 1201. ACS Symposium Series, vol 1201. American Chemical Society. 2015; pp 119-183. doi:https://doi.org/10.1021/bk-2015-1201.ch003

Publisher's note Springer Nature remains neutral with regard to jurisdictional claims in published maps and institutional affiliations.